

# Parallel stochastic programming for energy storage management in smart grid with probabilistic renewable generation and load models

ISSN 1752-1416  
 Received on 19th August 2018  
 Revised 10th December 2018  
 Accepted on 11th January 2019  
 E-First on 14th February 2019  
 doi: 10.1049/iet-rpg.2018.5737  
 www.ietdl.org

Yue Wang<sup>1</sup> ✉, Hao Liang<sup>1</sup>, Venkata Dinavahi<sup>1</sup>

<sup>1</sup>Department of Electrical and Computer Engineering, University of Alberta, Edmonton, Canada

✉ E-mail: ywang15@ualberta.ca

**Abstract:** Renewable power generation combined with energy storage (ES) is expected to bring enormous economical and environmental benefits to the future smart grid. However, the ES management in smart grid is facing significant technical challenges due to the volatile nature of renewable energy sources and the buffering effect of ES units. The challenges are further complicated by the increasing size and complexity of the system, as well as the consideration of random usage patterns of electrical appliances by customers. To address these challenges, this study proposes a parallel decomposition method for large-scale stochastic programming in a distribution system with renewable energy sources and ES units. By leveraging nested decomposition, the problem can be converted into independent sub-problems with a series of time periods. In addition, the reformulated problem is fully parallel for speed up in execution. The performance of the proposed method is evaluated based on the IEEE 4-bus and 33-bus test distribution systems with real photovoltaic generation and electrical appliance usage data. The case study demonstrates that the proposed scheme can substantially reduce the system operation cost, with low computational complexity.

## Nomenclature

### Superscript

Bat	battery
ch, dch	charging/discharging process
$e, x$	customer power consumption and benefits
$f$	households
$g$	power grid
net	wholesale market
$R$	residence total power consumption
$r$	renewable power generation
$u$	utility

### Variables

$\eta$	probability distribution
$\mathcal{L}$	power loss
$\xi$	probability distribution
$c$	electricity price
$D$	battery degradation
$G()$	price-sensitive function
$H, h$	optimal cut variables
$I$	node current
$O()$	house occupied function
$P$	real power
$p$	probability
$Q$	reactive power
$S$	energy storage
$s$	complex power flow
$U$	constraints representative
$V$	node voltage
$Y$	admittance

### Sets and individuals

$A, a$	house appliances $a \in A$
$K, k$	scenarios $k \in K$
$M, m$	households $m \in M$
$N, n$	bus nodes $n \in N$

$T, t$	time slots $t \in T$
$Z, z$	house types $z \in Z$

## 1 Introduction

With increasing concerns about the environmental impacts of grid power, sustainable renewable generation units, especially photovoltaic (PV) panels, are being widely installed for their economical and environmental benefits. For example, the installation capacity of PV generation in Canada has reached 2517 MW in 2015, which is ten times more than that of 2010 according to [1]. As the abundance and environmental advantages of solar power are becoming perceptible, PV technology has been developed rapidly in recent years. However, due to the volatile nature of renewable energy, solar power output results in constant fluctuations in distribution systems. Therefore, how to deal with the PV panel power output to make the system economical and how to use renewable energy efficiently in distribution systems still require extensive research.

Recently, there are many studies on renewable energy applications in the distribution system. Energy storage (ES) is usually integrated with renewable generation to improve the reliability and efficiency of the power grid [2, 3]. Energy management system (EMS) integrates the renewable generation and ES is invested in [4–8]. Specifically, to maximise utility for the demands with uncertain distributed renewable energy and customers' power demand, Rahimiyan *et al.* in [4] propose a robust optimisation algorithm, which allows the customer to operate at a suitable time. In [5], an ES system (ESS) is introduced against the uncertainties, which helps the EMS to produce an economical and reliable microgrid dispatch. A hierarchical EMS architecture is proposed in [6], which consists of load demand forecasting and renewable generation resource integration, aiming at achieving optimal scheduling of power generation resources in a smart grid. Romero-Quete and Cañizares in [7] proposed an affine arithmetic method for EMS in isolated microgrids. In this model, uncertain load and renewable energy are managed through robust commitment and dispatch, and all of the possible realisations are within the predetermined uncertain range. EMS in [8] is designed

for both grid-connected mode and isolated mode, and the proposed robustness solution is compared with the Monte Carlo simulation. However, the optimal operation of the EMS in these research works typically treats the customer's home demand as an integral part of a random value in the distribution system.

Moreover, considering the investment and maintenance cost of the household battery, a relatively high-capacity storage system in a specific area such as a community, accessible by a group of houses, is more preferable. Such batteries can be shared among these houses instead of the private battery for each home, and take advantage of reducing the cost of investment, operation and maintenance by each end user [9, 10]. They can also mitigate the negative impact of the randomness of renewable generation and load on distribution system reliability. Residential optimal EMSs with renewable power generation units are proposed by Rastegar *et al.* [11], Mediawaththe *et al.* [12], Li *et al.* [13], Kwon *et al.* [14] and Zhu *et al.* [15]. Researchers treated multiple houses with controllable loads or distributed load groups in a smart grid to reduce the fluctuation of power flow caused by renewable energy [16, 17]. Some of the recent studies have taken a deterministic approach when dealing with the volatile properties of renewable energy [3, 11–13, 16]. In [2, 14, 15], the stochastic nature of renewable energy is considered and characterised based on historical data or the worst case [17]. These methods can be categorised as the scenario-based approach. However, the random features of both the renewable energy and the household power consumption should be taken into account by all scenarios.

Different from recent studies, this paper focuses on a distribution system in which households are equipped with renewable energy and community shared ES units. Along with the ES units, households can flexibly interconnect with a distribution system for electricity supply and demand. This paper considers the highly random features of PV power output and household electrical consumption. Hence, we solve the problem via stochastic programming and implement parallel decomposition to transfer the large-scale problem into a series of independent sub-problems. Accordingly, the reformulated problem can be fully paralleled.

Specifically, the main contributions of this work are summarised as follows:

- i. In this work, both PV power generation and household electrical consumption are characterised via probabilistic models. Notably, the PV power probabilistic model is derived from solar irradiance, and the model of residential power consumption is based on a bottom-up approach, which is formulated from customers' random usage patterns. To better approximate real cases, various types of residential loads are considered.
- ii. We proposed a novel problem formulation for optimal ES management. In this formulation, the cost of the distribution system not only considers battery operation cost, but also incorporates the household uncertain load demand and the PV generation electric profit based on a probabilistic model.
- iii. To address the technical challenges introduced the probabilistic PV generation and load models, a parallel computing method based on nested decomposition is developed to reduce the computational complexity.
- iv. Extensive simulations are conducted to evaluate the performance of the proposed method, based on the IEEE 4-bus and 33-bus test distribution systems with real PV generation and electrical appliance usage data.

The rest of this paper is organised as follows. The existing literature is reviewed in Section 2. In Section 3, the system model which includes distributed linear power flow, probabilistic PV generation model, ES model and probabilistic residential load models are introduced. In Sections 4 and 5, the problem formulation and parallel decomposition approach for stochastic programming in the distribution system are presented, respectively. In Section 6, we use the IEEE 4-bus and 33-bus test distribution systems to evaluate the effectiveness of the proposed method, followed by the concluding remarks in Section 7.

## 2 Related work

In the existing literature, the random features at both distribution system and residential customer levels have been widely studied [18–26]. At the distribution system level, uncertain loads are considered in optimal power flow in [18], and energy management problems for grid-connected microgrids under uncertainties such as random renewable generation and loads are proposed in [19, 20]. Also, transmission network expansion planning problem under these uncertainties is proposed in [21]. A distribution network configuration optimisation problem with uncertainties is investigated in [22]. Both works use a robust optimisation approach to solve the formulated problems. These works are based on distribution system level study, and random facility usages are characterised by the worst case. In other words, these methods are based on a deterministic approach.

At the residential customer level, a stochastic bottom-up analytical model is designed to describe the domestic electrical load profiles in [23, 24]. The home energy management system (HEMS), which consider the uncertainties of household appliance usage and renewable generation units, aiming to seek the minimum household electricity bills, are proposed in [25, 26]. Similar to the research work at the grid level, the fundamental idea is to describe the stochastic features via deterministic model or Monte Carlo simulations at the residential level or use the robust optimisation approach, which relies on the upper and lower bounds of uncertain variables to solve the optimisation problem.

To improve the performance of energy management schemes, all the random scenarios of electrical appliance usage patterns should be considered. However, the scenario set is too massive to be simulated efficiently. Yet, large-scale scenario characterisation and reduction in distribution systems are still challenging tasks.

To address such massive set of scenarios, most recent studies utilise the robust approach [18, 20–22, 26, 27], chance constrained programming [19] and Monte Carlo simulation [28]. Table 1 gives a brief summary of these references. It is notable that in these recent research works, the randomnesses of renewable generation and households demand are discussed. However, these approaches either apply specific scenarios or use the worst case for simulation, which can also be classified as deterministic (D) approaches (compare to stochastic (S) approach).

On the other hand, to accelerate solution procedure, parallel computing [29–31] and decomposition algorithm [32, 33] are widely used to solve large-scale problems. Using parallel computing technique, we can first decompose the optimisation problem into multiple sub-problems or scenarios, and then implement computing so that each core (thread) solves one sub-problem or one scenario to speed up in the execution process. A scenario-based decomposition method is developed to address the multiobjective stochastic economic dispatch problem [32]. In [33], a new nested Benders decomposition strategy is presented to solve a multi-period problem for hydrothermal scheduling.

Our work aims to minimise system loss in the distribution system via a parallel decomposition algorithm, based on the probabilistic renewable generation and load models. Different from the existing research, this work considers the probabilities of all scenarios and solves the problem by stochastic programming. Moreover, the residential system consisting of different house types comprises the holistic configuration of the distribution system. By leveraging the proposed parallel decomposition algorithm, the massive scenario set can be efficiently addressed and the computational time is reduced significantly.

## 3 System model

In this paper, we consider a typical distribution system composed of households equipped with renewable energy sources, manually controlled appliances with probabilistic usage patterns and shared ES units. In this section, we introduce the models of these components in the system.

**Table 1** Parts of references considering uncertainties

Reference	Methods	HEMS			Distribution			HEMS in dis			D/S	
		PV	A	ES	PV	A	ES	PV	A	ES		
[11]	two-point estimate method	✓	✓	✓							D	
[16]	tabu search method	✓	✓	✓							D	
[25]	roulette wheel mechanism	✓	✓	✓							D	
[12]	Stackelberg game	✓		✓							D	
[13]	routing algorithm	✓		✓							D	
[23]	semi-Markov process			✓							S	
[24]	bottom-up model (random case)			✓							D	
[26]	robust optimisation			✓							D	
[10]	bi-level optimisation						✓				D	
[9]	robust optimisation						✓	✓	✓		D	
[4, 8]	robust optimisation						✓		✓		D	
[3]	maximum power point tracking						✓		✓		D	
[7]	affine arithmetic method						✓		✓		D	
[6]	bi-level, imperialist competition algorithm						✓		✓		D	
[5]	two-stage stochastic programming						✓		✓		D	
[19]	chance constrained programming						✓	✓			D	
[20–22]	robust optimisation						✓	✓			D	
[28]	approximate dynamic programming and Monte Carlo simulation						✓	✓			S	
[18]	robust transient stability constrained							✓			D	
[2]	two-period stochastic programming (historical data)								✓	✓	✓	D
[14]	approximate dynamic programming (expected value)								✓		✓	D
[15]	graphical capacity selection method								✓		✓	D
proposed work	parallel decomposition algorithm								✓	✓	✓	S

**3.1 Distribution system model**

For an  $N$  node system, the complex power flow  $s_n$  on the node  $n$  consists of real power  $P_n$  and reactive power  $Q_n$  and equals to the product of voltage  $V_n$  and the conjugate of the corresponding nodal current  $I_n$ . In this work, we denote subscript  $\{0, 1, \dots, n\}$  as the set of nodes and node 0 as the slack node. Therefore, the complex power flow can be represented as

$$s_n = P_n + jQ_n = V_n I_n^* \tag{1}$$

The current  $I$  is linearly related to bus voltage  $V$  via the nodal admittance matrix  $Y$ , which can be formulated as  $I = YV$ . In [34], Bolognani and Zampieri proposed a linear approximation of the power flow solution by assuming that all the shunt admittances at the buses are negligible, by using the vector of all ones  $\mathbf{1}$ , we have the following relation of nodal admittance matrix  $Y$ :

$$Y\mathbf{1} = \mathbf{0} \tag{2}$$

Moreover, by partitioning the admittance matrix  $Y$  between two nodes 0 and  $n$ , we rewrite the linear relation between current and voltage as

$$\begin{bmatrix} I_0 \\ I_n \end{bmatrix} = \begin{bmatrix} Y_{00} & Y_{0n} \\ Y_{n0} & Y_{nn} \end{bmatrix} \begin{bmatrix} V_0 \\ V_n \end{bmatrix} \tag{3}$$

Through this relation and (2), the voltage can be solved linearly by using the following equation:

$$V_n = V_0 \mathbf{1} + Y_{nn}^{-1} I_n \tag{4}$$

where  $Y_{nn}$  is invertible because  $\mathbf{1}$  is the only vector in the null space of  $Y$ . Consequently, power loss can be calculated as

$$\mathcal{L}_n = Y |V_n|^2 \tag{5}$$

**3.2 Probabilistic model of PV generation**

In this work, we use solar irradiance to compute the power output of a PV array. Solar irradiance  $I_\beta$  can be derived from the PV array inclination angle  $\beta$  as follows [35]:

$$I_\beta = \left[ \left( R_b + \rho \cdot \frac{1 - \cos \beta}{2} \right) + \left( \frac{1 + \cos \beta}{2} - R_b \right) \cdot p \right] I_o \cdot k_t - \left( \frac{1 + \cos \beta}{2} - R_b \right) \cdot q \cdot I_o \cdot k_t^2 \tag{6}$$

where  $R_b$  is the ratio of beam radiation on a leaned PV array surface to that on a horizontal surface. The calculation of  $R_b$  can be found in [36], where  $\rho$  is the reflectance of the ground. The extraterrestrial solar irradiance is indicated by  $I_o$ , which can be calculated as

$$I_o = r_d \cdot \frac{H_o}{3600} \tag{7}$$

where  $r_d$  is the correlation between the diffuse radiation in a day and  $H_o$  is the extraterrestrial total solar radiation on a horizontal surface introduced by Orgill and Hollands [37].

In (6),  $p$  and  $q$  are the parameters describing the relationship between the diffuse fraction  $k$  and the clearness indicator  $k_t$  as  $k = p - qk_t$ , where the subscript  $t$  indicates the time and  $k_t$  is the hourly clearness index which is an uncertain variable to model the random behaviour of the terrestrial solar radiation. The probability density function (PDF) of  $k_t$  is introduced in [38].

The PDF of PV active power output is presented in [39]. As a result, the PDF of PV generation can be determined by the PDF of solar irradiance. Specifically, the relationship between random variable  $k_t$  controlled solar irradiance and PV active power output can be described linearly as

$$P_{m,t}^r = I_{\beta,t} A_m \eta (1 - \rho(T - T_{ref})) \tag{8}$$

where  $P_{m,t}^r$  is the PV active power output from the household  $m$  at a time  $t$ ,  $I_{\beta,t}$  is the actual irradiance,  $A$  is the total area of the PV

array,  $\rho$  is the short-circuit temperature coefficient and  $T$  and  $T_{ref}$  are practical and reference temperature coefficients, respectively. According to Tan *et al.* [40], the variation in solar irradiance will ultimately result in a change in the cell temperature. However, the change of PV cell temperature is much slower than the rapid diversification of solar irradiance and thus is not considered in this paper. Therefore, the relationship between the PV generation and solar irradiance is given by

$$P_{m,t}^r = I_{\beta,t} A_m \eta. \quad (9)$$

The PDF of solar irradiance is denoted as  $g_{I_{\beta}}(I_{\beta,t})$ . Then, the PDF of the PV power output  $\xi_{m,t}^r(P_{m,t}^r)$  can be calculated and is defined as

$$\xi_{m,t}^r = g_{PV}(P_{m,t}^r). \quad (10)$$

### 3.3 ES model

In this work, we consider a typical distribution system where shared batteries are used as ES devices. For a specific node  $n \in N$  with battery ES device, the energy stored  $S_{n,t}$  at a time  $t$  is limited by a minimum value  $\underline{S}_{n,t}$  and maximum value  $\overline{S}_{n,t}$  as follows:

$$\underline{S}_{n,t} \leq S_{n,t} \leq \overline{S}_{n,t}. \quad (11)$$

To extend battery life, we also limit the charging and discharging power by

$$\begin{aligned} \underline{S}_{n,t}^{ch} &\leq S_{n,t}^{ch} \leq \overline{S}_{n,t}^{ch}, \\ \underline{S}_{n,t}^{dch} &\leq S_{n,t}^{dch} \leq \overline{S}_{n,t}^{dch}, \end{aligned} \quad (12)$$

where the underscore values indicate lower limits, and the over-line ones are the upper limits. The superscripts ch and dch denote battery charge and discharge, respectively.

Furthermore, considering the battery efficiency, the power drawn from or injected to the grid when the battery is charging or discharging, respectively, can be calculated as

$$\begin{aligned} S_{n,t}^{ch} &= P_{n,t}^{ch} / (1 - \rho^{ch}), \\ S_{n,t}^{dch} &= P_{n,t}^{dch} \cdot (1 - \rho^{dch}), \end{aligned} \quad (13)$$

where  $P^{ch}$  and  $P^{dch}$  indicate charging and discharging powers, respectively; Coefficients  $\rho^{ch}$  and  $\rho^{dch}$  represent charging efficiency and discharging efficiency, respectively.

Moreover, due to the limited life spans of batteries, we should consider the battery degradation  $D$  [41] caused by the multi-time charging or discharge in daily usage

$$D_{n,t} = \frac{u \cdot S_{n,t}^{avg} - v}{CF \cdot 15 \cdot 8760}, \quad (14)$$

where  $u$  and  $v$  are linear fitting parameters, while CF is the battery capacity fade (CF) at the end of the life. These three parameters depend on the type of battery. In addition,  $S^{avg}$  is the average stored power level.

### 3.4 Probabilistic model of loads

In this work, a bottom-up approach [42] is implemented to model the residential loads in a distribution system. The household daily time of use (ToU) probability profiles is used to infer the appliance operation probability. The ToU probability profiles may vary with house types, for which the composition is shown in Table 2.

All the household electrical usages are classified depending on whether they have electric heating or not, and holidays or workdays [43]. We represent the household daily ToU probability distribution by  $\xi_{m,a,t}$ . The subscripts  $(m, a, t)$  denote the index of

**Table 2** Composition of households in the UK (2001 census)

single pensioner household (65+ years old)	14%
single non-pensioner household	16%
multiple pensioner household	9%
household with children	29%
multiple person household with no dependent children	31%

houses, different household appliances and time slots, respectively. It is assumed that the devices related to an identical activity are following the same probability. For example, cooking-related electrical appliances such as blender, toaster, coffee maker and microwave oven follow the distribution of cooking. On the other hand, washer and dryer follow the distribution of laundry.

The influence of electric price on ToU probability distribution profiles of different activities is also distinct. For example, the probability distribution related to entertainment is price insensitive, as the customers are reluctant to change their behaviour for the sake of saving money. On the other hand, activities such as washing machine and dryer are sensitive to price due to low human intervention. Such properties can be introduced as price-sensitive function  $G(W_t)$ . Therefore, a price-sensitive residence ToU probability distribution profile can be expressed as

$$\xi_{m,a,t}' = G(W_t) \cdot O(m, t) \cdot \xi_{m,a,t}, \quad \forall m \in M, a \in A, t \in T. \quad (15)$$

In this equation,  $O(m, t)$  denotes the occupation function, which can be used to model different schedules of the residents in various houses, or describe holidays or workdays, as follows:

$$O(m, t) = \begin{cases} 1, & \text{when the house is occupied,} \\ 0, & \text{when the house is unoccupied,} \end{cases} \quad \forall m \in M. \quad (16)$$

After implementing the price-sensitive function or household occupied function to the original distribution, because of the property of the price-sensitive function, the summation of the adjusted probability distribution  $\xi_{m,a,t}'$  is usually smaller than or equal to 1. Therefore, a calibration (normalised) equation is introduced as follows:

$$\xi_{m,a,t}'' = \frac{\xi_{m,a,t}'}{\sum_t \xi_{m,a,t}'}. \quad (17)$$

Consequently, household power level distribution for time  $t$  can be derived through ToU probability and appliance rated power consumption. For appliance  $a \in A$  operation scenarios at a time  $t$ , the total number of power level scenarios which might be happening is  $K$  excluding the repeated power levels (i.e. this number will be  $2^A$  if there is no recurrence). First, we assume that there is no recurrence and the power level subscript is  $l \in \{1, 2, \dots, 2^A\}$ . For a specific power level  $P_{m,l,t}$ , the corresponding probability  $\zeta_{m,l,t}$  is given by

$$\zeta_{m,l,t} = \prod_A \xi_{a',t}' \cdot \xi_{a,t}', \quad \forall a \cap a' = A. \quad (18)$$

Here,  $\xi_{a',t}'$  indicates the turn-on appliance probability and  $\xi_{a,t}'$  denotes the turn-off appliance probability. Then, we can remove the repeated levels by adding the probabilities of the same power level together

$$\zeta_{m,k,t}^f = \sum_l \zeta_{m,l,t}, \quad \forall P_{m,k,t}^f = P_{m,l,t}, l \in \Omega_k. \quad (19)$$

The set  $\Omega_k$  represents the set of all appliance operation scenarios with the same power level  $k$ . Therefore, the probability distribution of a power level can be represented as

$$\zeta_{m,k,t}^f = g_{PV}(P_{m,k,t}^f). \quad (20)$$

Considering the exponential growth of the number of power levels when adding more electrical appliances, we can reorganise the existing power levels by reducing the degree to  $y_l$ , given by

$$P_{m,k,t}^f(y_l) = \frac{\max(P_{m,k,t}^f)}{l}, \quad \forall y_l = 1, 2, \dots, \quad (21)$$

where  $l$  is the length of power interval and the corresponding probability is the summation of the probabilities in the interval as

$$\zeta_{m,k,t}^f(y_l) = \sum_{\tau} \zeta_{m,k,t}^f \cdot \quad (22)$$

By combining these power levels, we should note that if a shorter length is chosen, the accuracy of the reorganised power levels will be higher, but the execution time will be long at the same time.

#### 4 Problem formulation

Generally, decisions on shared ES management in distribution systems are made to either minimise system loss or maximise profit. The former formulation is adopted in this paper. In this case, since the utility has the permit to operate the battery to indirectly control the customer's home load demand; therefore, the battery degradation cost should consider as the system cost. Moreover, another system operation loss such as power loss and electricity power benefit is considered in our objective function, due to these costs are related to the storage operation. Some losses such as investment and maintenance costs are usually at a fixed rate, so they are excluded from the total system cost. Therefore, we include the power losses, shared ES degradation cost and electrical profit in the objective function, which is given by

$$\begin{aligned} \min_D C^g &= \sum_{n,t} c_t^{\text{net}} E(\mathcal{L}_{n,t}) + c_t^{\text{bat}} E(D_{n,t}) \\ &+ \sum_{n,m,t} (c_t^{\text{net}} - c_t^x) E(P_{n,m,t}^{R,x}) + \sum_{n,m,t} c_t^e E(P_{n,m,t}^{R,e}) \\ &= \sum_{n,t} (c_t^{\text{net}} \sum_k p^{\mathcal{L}}(k) \mathcal{L}_t(k) + c_t^{\text{bat}} \sum_k p_t^d(k) (D_t(k))) \quad (23) \\ &+ \sum_m (c_t^{\text{net}} - c_t^x) \sum_k p_m^{R,x}(k) (P_m^{R,x}(k)) \\ &+ \sum_m c_t^e \sum_k p_m^{R,e}(k) (P_m^{R,e}(k)), \end{aligned}$$

where  $C^g$  are the total losses in the distribution system. With different superscripts,  $c_t$  represents time-varying electrical price,  $c_t^{\text{net}}$  indicates the electrical cost from the wholesale market,  $c_t^{\text{bat}}$  denotes the battery degradation cost, while  $c_t^x$  or  $c_t^e$  represents the price that utility sells to or purchases from customers, respectively. In the objective function, the first term shows the power loss caused by distribution system operation, and the value can be calculated from the power flow analysis (5). The second term is the cost of battery degradation, which is introduced in (14). The next term indicates the profit that utility earned via distributing electricity to the customers. The last term is the cost that utility purchases electricity generated from household renewable energy sources or ES devices. The superscripts  $x$  and  $e$  for power  $P$  indicate the power household utilised or generated, respectively. Note that the variables  $P_{n,m,t}^{R,e}$  and  $P_{n,m,t}^{R,x}$  do not have values simultaneously, which is considered as one of the constraints in the optimisation problem. To embody the expectations in (23), the probability mass functions of power loss, customer power consumption and generation are required, which are indicated by  $p_t^{\mathcal{L}}$ ,  $P_{n,m,t}^{R,x}$  and  $P_{n,m,t}^{R,e}$ , respectively. The constraints of the energy management problem are given by

$$S_{n,t} = S_{n,t-\Delta t} + \sum_m P_{n,m,t}^R \cdot \Delta t + P_{n,t} \cdot \Delta t, \quad (24)$$

$$P_{n,m,t}^R = \begin{cases} P_{n,m,t}^r - P_{n,m,t}^f & \\ = \begin{cases} P_{n,m,t}^{R,e} & \text{if } P_{n,m,t}^r - P_{n,m,t}^f \geq 0, \\ P_{n,m,t}^{R,x} & \text{if } P_{n,m,t}^r - P_{n,m,t}^f < 0, \end{cases} \end{cases} \quad (25)$$

$$S_{n,t} \leq S_{n,t} \leq \overline{S_{n,t}}, \quad (26)$$

$$P_{n,m,t}^r + P_{n,m,t}^g + \text{avg}(P_{n,m,t}^S) = P_{n,m,t}^f, \quad (27)$$

$$P_{n,t}^S = (S_{n,t} - S_{n,t-\Delta t})/\Delta t,$$

$$P_{n,t} = \sum_m P_{n,m,t}^g, \quad (28)$$

$$\underline{P_{n,t}} \leq P_{n,t} \leq \overline{P_{n,t}}, \quad (29)$$

$$\underline{V_{n,t}} \leq V_{n,t} \leq \overline{V_{n,t}}. \quad (30)$$

Note that in the objective function (23), both power  $P_{n,m,t}^r$  and  $P_{n,m,t}^f$  are random variables which are specified by the corresponding probability distributions. Battery related charging and discharging operations, which depend on the battery state in the previous moment, is defined by (24). The current battery state  $S_{n,t}$  is the summation of the previous battery state  $S_{n,t-\Delta t}$ , total power consumption at the node  $\sum_m P_{n,m,t}^R$  and power exchanged  $P_{n,t}$  during the current state. In (25), the total local power consumption  $P^R$  is defined as the difference between renewable power generation  $P_{n,m,t}^r$  and domestic appliance consumption  $P_{n,m,t}^f$ . Different superscripts  $P_{n,m,t}^{R,e}$  and  $P_{n,m,t}^{R,x}$  represent extra power sent to the grid and insufficient power that must be purchased from the grid, respectively. In addition, battery charging and discharging operations are constrained by lower and upper limits shown in (26). For any moment  $t$ , the condition of power balancing is realised in (27), where the total power for a specific house includes renewable power generation, domestic appliance power consumption and the power supplied by the grid and shared storage. Here, we use average battery supplied energy for the single house power balance. Real power for each node in the power system can be obtained via (28), which is the summation over houses. Reactive power, as well as a real power that is utilised for computing the system power flow, can be derived from real power by power factors. Finally, the power limit and voltage limit are shown in (29) and (30), respectively.

By including renewable energy and storage devices, the values of variables  $P_{n,m,t}^g$  and  $P_{n,t}^S$  can be either positive or negative. For  $P_{n,m,t}^g$ , a positive value means that end users purchase power from the grid, while a negative value indicates end users sell extra electricity to the grid. A similar rule applies to the variable  $P_{n,t}^S$ , where a positive value indicates the battery is discharging, while negative value represents charging.

In summary, the optimisation problems of (23) are formulated with constraints (24)–(30). Variables involved are introduced in the system model. Solution procedure will be presented in the next section. Variables involved are introduced in the system model. Solution procedure will be presented in the next section.

#### 5 Parallel stochastic programming for problem solution

As the size of the proposed problem would increase dramatically when adding any of the random features in this work, we contemplated adding cuts or linear supports to manipulate the domain of the problem progressively. These cuts are piecewise linear approximations of the functions, and they can be obtained by the Lagrangian multiplier, which is the result of the linear programming. These cuts are also precise lower bounds and can make the algorithm achieve any degree of accuracy. Therefore, in the following part, to derive the feasible cut, we start with scenario analysis.

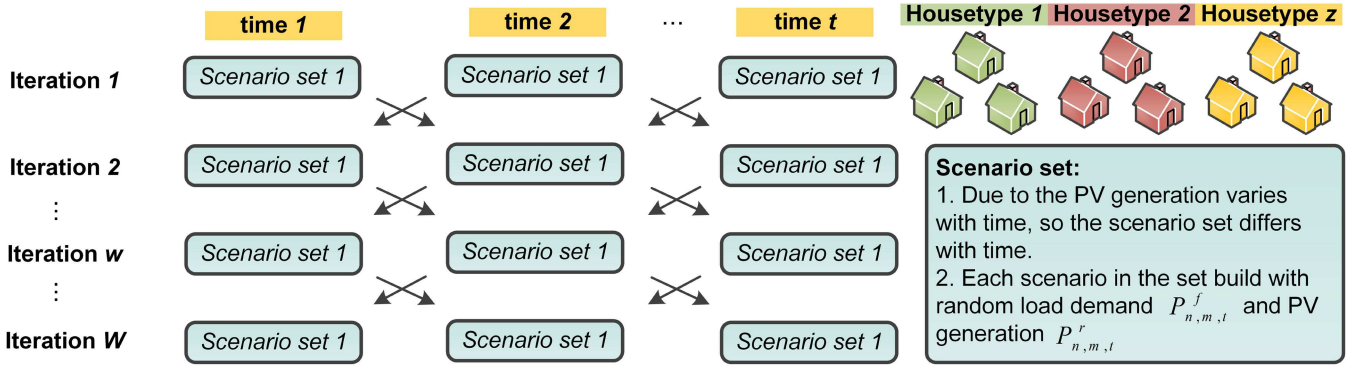


Fig. 1 Illustration of parallel stochastic programming

As shown in Fig. 1 and Table 2, houses can be divided into  $z$  types.

For each house type in each period, there exist  $k$  scenarios. A specific scenario is associated with random variables  $P_{n,m,t}^r$  and  $P_{n,m,t}^f$ , represents a combination of the values of renewable power generated from PV array and power consumption by residential electrical appliances, respectively. Consequently, an evaluation function for each scenario can be expressed as a cost function  $C_t^{g,(i,j)}(\mathcal{L}_{n,t}, P_{n,m,t}^R, D_{n,t})$ , which can be modelled as a dynamic programme with  $T$  stages. Therefore, for each period  $t$ , the cost function can be calculated as the current expenditure and future period  $t + \Delta t$  possible expenditure, given by the equation below: (see (31)).

In this modified objective function by each scenario, the superscript  $d$  indicates the descent/offspring situations of the current scenario for the next period  $t + \Delta t$ . Moreover, the constraints of each scenario can be concluded from the battery state  $S_t^{i,j}$  as follows:

$$S_t^{i,j} = S_{t-\Delta t}^{i,j} + \sum_m P_{n,m,t}^R (P_{n,m,t}^r(i), P_{n,m,t}^f(j)) \mathbf{1}(\Delta t) + P_{n,t}(i, j)(\Delta t), \quad (32)$$

where we assume the PV array power output is the same in an equivalent area, and the rank of  $\mathbf{1}$  matrix is equal to the number of total house types to make sure all the matrices are at the same rank. Concerning that the battery state  $S_t^{i,j}$  is related to a former state  $S_{t-\Delta t}^{i,j}$ , this process can be called the forward pass. Consequently, for each house  $m$ , the power exchange should satisfy

$$P_{n,m,t}^r(i) + P_{n,m,t}^g(i, j) + \text{avg}(P_{n,m,t}^S(i, j)) = P_{n,m,t}^f(j). \quad (33)$$

On the basis of battery charging and discharging rate limits and battery energy state constraint, we have

$$\frac{P_{n,t}^{S,(i,j)}}{S_{n,t}^{i,j}} \leq \frac{P_{n,t}^{S,(i,j)}}{S_{n,t}^{i,j}} \leq \frac{P_{n,t}^{S,(i,j)}}{S_{n,t}^{i,j}}, \quad (34)$$

$$\frac{S_{n,t}^{i,j}}{S_{n,t}^{i,j}} \leq \frac{S_{n,t}^{i,j}}{S_{n,t}^{i,j}} \leq \frac{S_{n,t}^{i,j}}{S_{n,t}^{i,j}}.$$

Then, the real power at a node  $n$  of the distribution system can be calculated as

$$P_{n,t}^g(i, j) = \sum_m P_{n,m,t}^g(i, j) = \sum_m [P_{n,m,t}^f(j) - P_{n,m,t}^r(i) - P_{n,m,t}^S(i, j)]. \quad (35)$$

The real power limit and voltage limit are shown as (36), where the nodal voltage can be calculated based on (3) in the former section

$$\frac{P_{n,t}^g(i, j)}{V_{n,t}(i, j)} \leq \sum_m \frac{P_{n,m,t}^g(i, j)}{V_{n,t}(i, j)} \leq \frac{\overline{P_{n,t}^g(i, j)}}{\overline{V_{n,t}(i, j)}}, \quad (36)$$

$$\underline{V_{n,t}(i, j)} \leq V_{n,t}(i, j) \leq \overline{V_{n,t}(i, j)}.$$

In addition, the line current can be derived from

$$s_{n,t}(i, j) = P_{n,t}^g(i, j) + jQ_{n,t}^g(i, j) = V_{n,t}(i, j)(I_{n,t}(i, j))^* = (V_0 \mathbf{1} - Y_{nn}^{-1} I_{n,t}(i, j))(I_{n,t}(i, j))^*. \quad (37)$$

Since the problem needs to be solved by the previous state, this process can be named as single scenario forward pass analysis. As we revealed at the beginning of this section, adding cuts or linear supports can achieve an accurate result, and the process of the algorithm can be accelerated.

A feasible cut can be built as [44]

$$H_t^{l,i,j} P_t^S(i, j) + h_t^{l,i,j} \geq 0, \quad (38)$$

where  $H_t^{l,i,j}$  and  $h_t^{l,i,j}$  can be calculated as

$$H_t^{l,i,j} = \mu_{t+\Delta t}^d \times [P_{n,m,t}^f(j) - P_{n,m,t}^r(i) - P_{n,m,t}^S(i, j)], \quad (39)$$

$$h_t^{l,i,j} = \mu_{t+\Delta t}^d \times 1 + \sum_j (\lambda_{t+\Delta t}^d \times U(i, j)),$$

where  $\mu$  and  $\lambda$  are the Lagrangian multipliers corresponding to each constraint. We use  $U(i, j)$  to represent all other constraints. The proposed nested decomposition algorithm for stochastic

$$C_t^{g,(i,j)}(\mathcal{L}_{n,t}, P_{n,m,t}^R, D_{n,t}) = C_t^g(\mathcal{L}_{n,t}, P_t^r(i), P_t^f(j), D_{n,t}) + E[C_{t+\Delta t}^g(\mathcal{L}_{n,t+\Delta t}, P_{t+\Delta t}^r(i), P_{t+\Delta t}^f(j), D_{n,t+\Delta t})] = c_t^{\text{net}} \mathcal{L}_{n,t}(i, j) + c_t^{\text{bat}} D_{n,t}(i, j) + (c_t^{\text{net}} - c_t^x) P_{n,m,t}^{R,x}(P^r(i), P^f(j)) + c_t^e P_{n,m,t}^{R,e}(P^r(i), P^f(j)) + \sum_{d \in \mathcal{D}_t^{i,j}} P_{t+\Delta t}^d(i, j) \cdot [c_{t+\Delta t}^{\text{net}} \mathcal{L}_{n,t+\Delta t}(i, j) + c_{t+\Delta t}^{\text{bat}} D_{n,t+\Delta t}^d(i, j) + (c_{t+\Delta t}^{\text{net}} - c_{t+\Delta t}^x) P_{n,m,t+\Delta t}^{R,x,d}(P^r(i), P^f(j)) + c_{t+\Delta t}^e P_{n,m,t+\Delta t}^{R,e,d}(P^r(i), P^f(j))]. \quad (31)$$

```

1: Set  $t = 1, w_1(i, j) = 1$ , solve optimization problem (31)-(37)
2: for  $t \in T$  do
3:   if  $t = 1$  and problem infeasible then
4:     STOP.
5:   else if the problem is feasible then
6:     apply optimal solution  $P_{opt}^{S, w_t}(i, j)$  to next time  $t + \Delta t$  to
       the problem (31). And  $w_t = w_t + 1, t = t + \Delta t$ .
7:     if any  $t + \Delta t$  problem is infeasible and (40) then
8:       add (38) to (31), let  $t = t - \Delta t$ .
9:     else if any  $t + \Delta t$  problem is infeasible with condition (40)
       then
10:      solve a finite sequence of sub-problems until one is
        feasible.
11:      if feasible, then
12:        a new set of values for  $t \in T$ , update results.
13:      end if
14:    end if
15:    else if all the sub-problems are infeasible, then
16:      STOP. The entire problem is infeasible.
17:    end if
18:  end for

```

Fig. 2 Algorithm 1: nested decomposition for stochastic programming

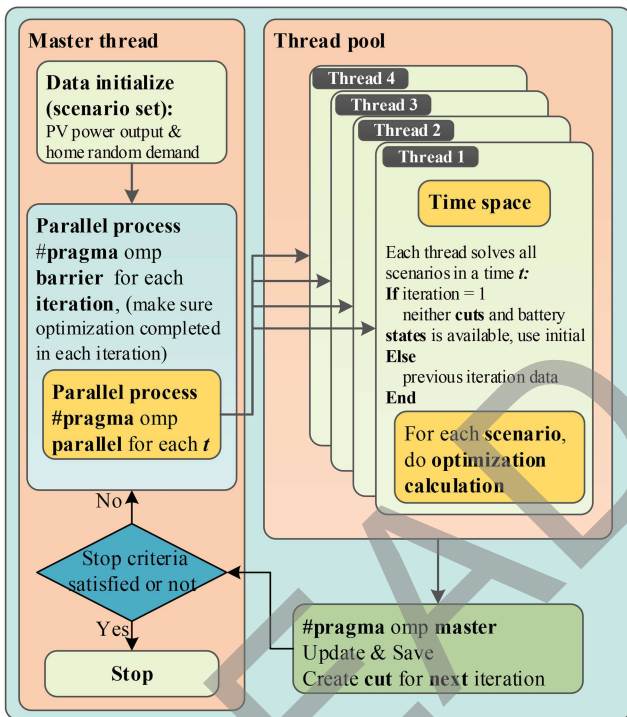


Fig. 3 Flowchart for the implementation of the nested decomposition parallel processing

programming is shown in Algorithm 1 (Fig. 2), with the details being described as follows:

- i. First, we set the time index  $t = 1$  and iteration index  $w = 1$ . Solve the current problem (31)–(37). If infeasible and  $t = 1$ , then stop; problem (23) is infeasible.
- ii. Otherwise, calculate the current time  $t$  optimal solutions for scenarios  $i \in \mathcal{I}_t$  and  $j \in \mathcal{J}_t$ . Solve (31) for next time and all scenarios applying the appropriate ancestor optimal solutions in (32). Moreover, go to the next iteration and time period.
- iii. If any period problem is infeasible and

$$H_t^{l, i, j} P_{n_t}^{S, (i, j)} + h_t^{l, i, j} < 0, \quad (40)$$

add a feasibility constraint to the corresponding ancestor period problem. Return to step 3.

- iv. Otherwise, iteratively solve a finite sequence of sub-problems (backward from  $t = T$  to  $t = 1$ ) until one is feasible. If a

Table 3 Characteristics of typical household appliances

Appliance category and name	Average power consumption, W	Average operation duration, h	Power factor
kitchen			
blender	175	0.2	0.73
coffee maker	900	0.4	1
deep fryer	1500	0.267	1
dishwasher	1300	0.667	0.99
food freezer	350	8	0.8
microwave oven	1500	0.333	0.9
range and oven	4000	0.833	1
toaster	1200	0.133	1
laundry			
dryer	5000	0.933	0.99
iron	1000	0.4	1
washing machine	500	0.867	0.65
entertainment			
computer (desktop)	250	8	0.8
computer (laptop)	30	8	0.8
laser printer	600	2	—
stereo	120	4	—
television	100	4.167	0.8
comfort and health			
air conditioner	750	2.467	0.9
electric heating	1000	8.333	1
fan	120	0.2	0.87
lights	60	8	0.93
vacuum cleaner	1300	0.333	0.9

problem is feasible, then one has a new set of values for each stage to ensure feasibility from period 1 through all the periods.

For a better understanding of the procedure, Fig. 3 describes the implementation of the proposed nested decomposition parallel processing using OpenMP. In this figure, data initialised from the master thread (core), by implementing barrier construct, we assign each thread processes one time slot. After the optimisation process by each thread, the results are sent to the master thread for data update and build cuts for the next iteration.

## 6 Case study

To demonstrate the effectiveness of parallel stochastic programming, we applied the proposed method on the IEEE 4-bus and 33-bus test distribution systems. The simulations are conducted on a Windows desktop with an Intel Core i7-4790 central processing unit at 3.60 GHz with 16 GB random access memory (four physical cores and eight logical cores), and all the experiments are performed in C++. The sub-problem of linear programming is solved via the Lpsolve library [45].

We first describe the configuration of the studied microgrid and relevant datasets and then present the simulation results and discussion. The microgrid energy management is implemented over a finite time horizon (e.g.  $T = 24$  h) in this paper and the time step is set to be 1 h. In Table 3 [46], we show the household appliance properties such as the average power consumption, the average operation duration and the power factor. The categories of typical household types were introduced in the previous section (Table 2); Different combinations of electrical appliances may lead to different electrical usage probabilities. Also, for the purpose of simulating closer to the real cases, we assume 40% of houses are equipped with renewable generation, and each bus equipped with the size of 30% capacity of the node power battery storage [47].

The wholesale market electrical pool price is obtained from Hourly Ontario Energy Price in April 2018 [48]. The ToU

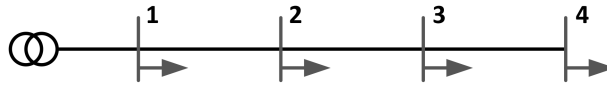


Fig. 4 One-line diagram of IEEE 4-bus test distribution system

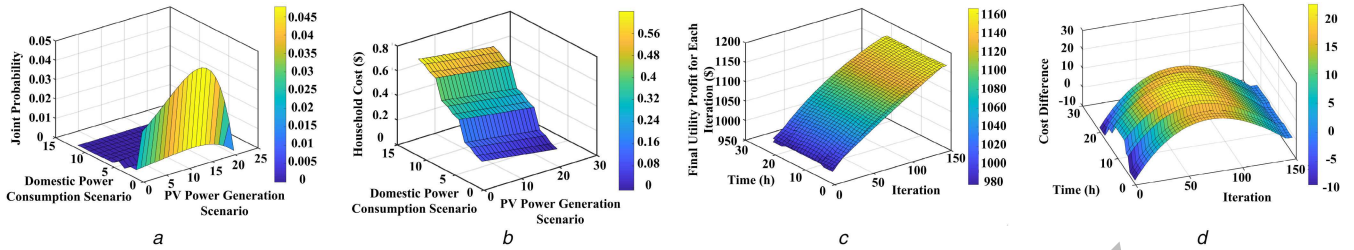


Fig. 5 Results for

(a) Probability distribution of domestic power consumption and renewable generation at 7 pm, (b) Household cost of the random set at 7 pm, (c) Convergence of final utility cost for each iteration, (d) Cost difference of two algorithms

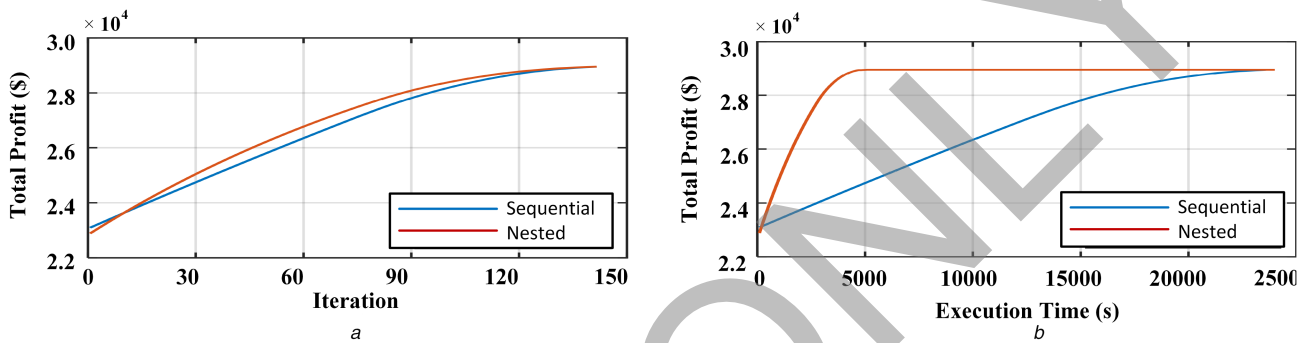


Fig. 6 Utility electrical profit results plotted against (best viewed in colour online)

(a) Number of iterations, (b) Execution time

electrical price for the customer is given in [49]. The feed-in tariff programme encourages customers to sell renewable energy to the grid, and the details can be found in [50].

### 6.1 IEEE 4-bus test distribution system

The first case study is performed on the IEEE 4-bus test distribution system. This 12.47 kV radial distribution system has a total peak load of 6000 kVA. The detailed data are available in [51], and the one-line diagram is shown in Fig. 4. A household with children is considered in this case. Owing to the relatively small scale of the distribution system which has a low computation complexity, we can evaluate our proposed scheme extensively by performing comparison under various system configurations.

As we introduced in the former section, two random factors, renewable PV power output and household electrical consumption are considered in this paper. Their joint probability distributions, which describe the stochastic properties of these two random variables, are shown in Fig. 5a. In this case, 21 PV generation and 12 energy consumption power levels are considered, which lead to 252 realisations in total. As we can see, section along the axis of domestic power consumption scenario shows the probability distribution of energy consumption with a specific PV power generation. On the other hand, the perpendicular section displays the PV power generation profile with a certain scenario of domestic energy consumption.

Fig. 5b shows the household electrical expense corresponding to the probability distribution in Fig. 5a. For a higher renewable power output, the cost for each household is lower and vice versa. Then, these scenarios are solved by linear programming. Once the forward process is solved, the Lagrangian multiplier can be accessed and then utilised as the composition of feasible cuts which constrain the backward process. By implementing both the forward process and backward process, the execution time of the whole process can be reduced by half at least.

To better demonstrate the convergence of the whole process, Fig. 5c shows the total utility cost in 1 day. The two layers are a sequential process (upper) and nested parallel process (lower),

respectively. The cost difference between the two processes is shown in Fig. 5d. The result indicates that these two processes converge to the same value, which indicates that optimality can be achieved based on the proposed nested parallel decomposition method.

Fig. 6 shows the convergence curve of the total benefit for a whole day. We compare the convergence curve versus (a) number of iterations and (b) execution time, where the red and blue curves represent parallel and sequential optimisations, respectively. The processes are executed backward and forward alternatively in the sequential optimisation. However, the nested decomposition-based parallel computing is executed with four cores simultaneously. We can see that both of these two methods converge to the same final result, while the nested decomposition can save execution time significantly.

Moreover, household daily power consumption under ToU price and household daily electrical cost are shown in Figs. 7a and b, respectively. It can be seen that on the user side, the household power consumption is negatively correlated with the electrical rate. In other words, the optimised domestic power consumption decreases with the increasing of the electrical price.

To further demonstrate the efficiency of the proposed method, we compare it against the scenario-based parallel processing method [29–31] in this simulation. This process can also be accelerated by computing each scenario parallelly in one period, but the acceleration is only valid in each time block and cannot run across time horizon and use the results from the previous iteration as a warm start, which differs from the proposed parallel nested decomposition algorithm. The comparison results are shown in Table 4. To complete the comparison, the computation time of a sequential process with a single core is also shown. With a single core, sequential computing is more efficient than the scenario-based parallel computing and the nested decomposition-based parallel process due to the overhead involved in parallel processing. Even all the processes are assigned to only one core, parallel computing involves overhead such as task assignment, data communication and data synchronisation. However, with multiple

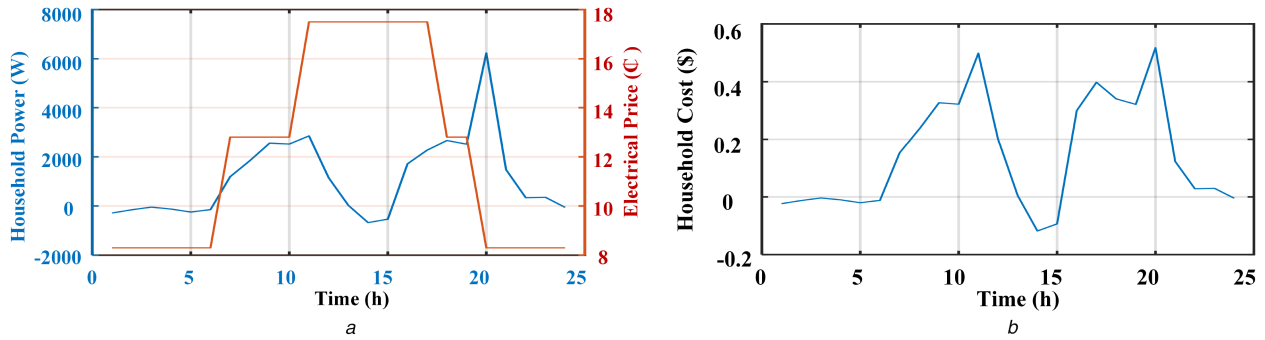


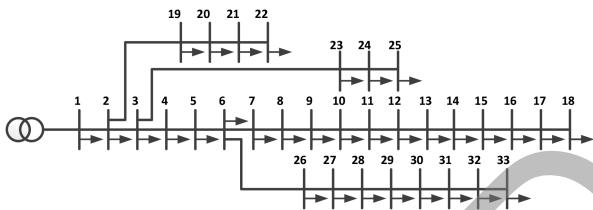
**Fig. 7** Final iteration result for (best viewed in colour online)  
 (a) Household daily electrical cost, (b) Household daily power consumption under ToU price

**Table 4** Execution time (s) for different numbers of cores

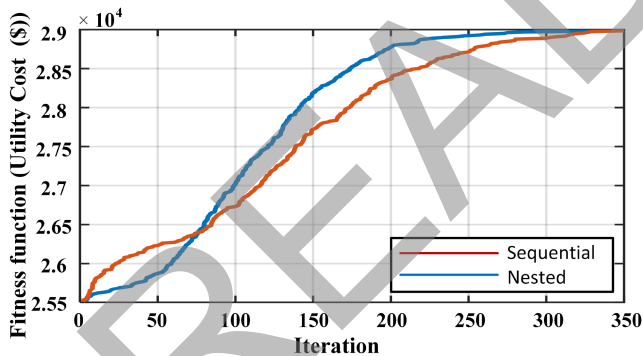
Number of cores	One core	Two cores	Three cores	Four cores
sequential run	19,254	n/a	n/a	n/a
scenario-based parallel	21,005	12,398	7251	6513
nested decomposition parallel	24,699	11,471	6871	5804

Number of cores	Five core	Six cores	Seven cores	Eight cores
sequential run	n/a	n/a	n/a	n/a
scenario-based parallel	4932	4277	3712	3682
nested decomposition parallel	4742	3966	3548	3494



**Fig. 8** One-line diagram of IEEE 33-bus test distribution system



**Fig. 9** Final utility electrical profit results plotted against the proposed nested parallel process and sequential process (best viewed in colour online)

cores, the execution time for the parallel process is drastically reduced with the increasing number of processors, which demonstrates its efficiency. Comparing the two parallel processes, the difference of the execution time is caused by the difference in the overhead for the parallel processes. The time for data communication and data synchronisation of the scenario-based parallel process is between scenarios, which is much more than that of the nested decomposition process, where the data communication and data synchronisation are between iterations.

### 6.2 IEEE 33-bus and 119-bus test distribution system

The IEEE 33-bus test distribution system (Fig. 8) is a 12.66 kV radial distribution system, and the total real and reactive power

loads on the system are 3715 kW and 2300 kVar, respectively. The test system data is available in [52]. All kinds of households introduced in Table 2 are added to this comprehensive simulation with their corresponding percentage. Still, there are a total 40% of houses equipped with renewable generation.

The sequential computing and the proposed nest decomposition-based parallel computing results are shown in Fig. 9. From this figure, we can observe that at first 80 iterations, sequential process has a better performance than the nested one, since the nested process is using results from the previous iteration while sequential process updates the results by the current iteration. Once the nested process obtains high-quality cuts, it will have a better performance than the sequential process.

The whole process for sequential simulation took 527,703 s, which is 6.108 days when the number of total scenarios is 9373, and the nested parallel process requires 144,189 s to converge, resulting in a speed up of 3.6598 times. Moreover, the IEEE 119-bus test distribution system is performed to test the scalability and effectiveness of the proposed model. The system is operated at 11 kV, and the total real and reactive loads are 22,709.7 kW and 17,041.1 kVar, respectively. The system data can be found in [53]. We implement scenario reduction to all the IEEE 4-bus, IEEE 33-bus and IEEE 119-bus test distribution system to test the scalability and efficiency of the proposed scheme.

In this simulation, the same number of total scenarios is chosen for all these three test distribution systems, with the total number of scenarios being 9373. PV power generation is assumed to be the same due to the same area. By combining the power level using (21) and (22), we can reduce the total scenario to shorten the execution time, while maintaining the accuracy of the proposed method, details can be found in [46]. Therefore, the results for execution time for a different number of scenarios are shown in Table 5. The execution time for 33-bus can be as low as 2 h compared with 6.108 days with sequential simulation. We can see that with the expansion of the network scale, the proposed solution can be effectively implemented with good scalability. Owing to the linear power flow analysis, we implemented in this work, the execution time is efficiently reduced even if the test system is large.

**Table 5** Execution time (s) for different number of scenarios and buses

Number of buses	Number of total scenarios			
	9373	938	468	234
4	70,363	11,227	7624	3316
33	144,189	22,608	9469	4633
119	189,265	28,176	15,149	6740

## 7 Conclusion

In this paper, we propose a parallel decomposition algorithm for stochastic programming in an electrical distribution system, which consists of household appliances, ESS and PV panels as renewable energy sources. The PV panel power output and household load demand are modelled by probabilistic models, for which a parallel computing method based on nested decomposition is developed to speed up the solution process for optimal energy management. The proposed method has been evaluated through two case studies, and the simulation results demonstrate the efficiency and accuracy of the proposed method. Furthermore, compared with the methods such as traditional sequential process or scenario-based parallel computing, the proposed method can achieve speed up in execution. In our future work, we will include EV random driving mode as another stochastic factor in the optimisation process. Owing to the high uncertainty of EV driving profile such as the uncertain departure time, driving distance and destination, more efficient parallel implementation is needed to improve the performance.

## 8 Acknowledgments

This work was supported by the Natural Sciences and Engineering Research Council of Canada (NSERC). Yue Wang was sponsored by the China Scholarship Council (CSC) under Grant no. 201406350066.

## 9 References

[1] International renewable energy agency. Available at <http://resourceirena.irena.org/gateway/dashboard/?topic=4&subTopic=18>, February 2016

[2] Wang, H., Huang, J.: 'Joint investment and operation of microgrid', *IEEE Trans. Smart Grid*, 2017, **8**, (2), pp. 833–845

[3] Yi, Z., Dong, W., Etemadi, A.H.: 'A unified control and power management scheme for PV-battery-based hybrid microgrids for both grid-connected and islanded modes', *IEEE Trans. Smart Grid*, 2018, **9**, (6), pp. 5975–5985

[4] Rahimiyan, M., Baringo, L., Conejo, A.J.: 'Energy management of a cluster of interconnected price-responsive demands', *IEEE Trans. Power Syst.*, 2014, **29**, (2), pp. 645–655

[5] Olivares, D.E., Lara, J.D., Cañizares, C.A., *et al.*: 'Stochastic-predictive energy management system for isolated microgrids', *IEEE Trans. Smart Grid*, 2015, **6**, (6), pp. 2681–2693

[6] Marzband, M., Parhizi, N., Savaghebi, M., *et al.*: 'Distributed smart decision-making for a multimicrogrid system based on a hierarchical interactive architecture', *IEEE Trans. Energy Convers.*, 2016, **31**, (2), pp. 637–648

[7] Romero-Quete, D., Cañizares, C.A.: 'An affine arithmetic-based energy management system for isolated microgrids', *IEEE Trans. Smart Grid*, 2018

[8] Giraldo, J.S., Castrillon, J.A., López, J.C., *et al.*: 'Microgrids energy management using robust convex programming', *IEEE Trans. Smart Grid*, 2018

[9] Zhang, C., Xu, Y., Dong, Z.Y., *et al.*: 'Robust operation of microgrids via two-stage coordinated energy storage and direct load control', *IEEE Trans. Power Syst.*, 2017, **32**, (4), pp. 2858–2868

[10] Tascikaraoglu, A., Paterakis, N.G., Erdinc, O., *et al.*: 'Combining the flexibility from shared energy storage systems and DLC-based demand response of HVAC units for distribution system operation enhancement', *IEEE Trans. Sustain. Energy*, 2019, **10**, (1), pp. 137–148

[11] Rastegar, M., Fotuhi-Firuzabad, M., Zareipour, H., *et al.*: 'A probabilistic energy management scheme for renewable-based residential energy hubs', *IEEE Trans. Smart Grid*, 2017, **8**, (5), pp. 2217–2227

[12] Mediwaththe, C., Stephens, E., Smith, D., *et al.*: 'Competitive energy trading framework for demand-side management in neighborhood area networks', *IEEE Trans. Smart Grid*, 2018, **9**, (5), pp. 4313–4322

[13] Li, J., Lin, X., Nazarian, S., *et al.*: 'CTS2M: concurrent task scheduling and storage management for residential energy consumers under dynamic energy pricing', *IET Cyber-Phys. Syst. Theory Appl.*, 2017, **2**, (3), pp. 111–117

[14] Kwon, S., Xu, Y., Gautam, N.: 'Meeting inelastic demand in systems with storage and renewable sources', *IEEE Trans. Smart Grid*, 2017, **8**, (4), pp. 1619–1629

[15] Zhu, X., Yan, J., Lu, N.: 'A graphical performance-based energy storage capacity sizing method for high solar penetration residential feeders', *IEEE Trans. Smart Grid*, 2017, **8**, (1), pp. 3–12

[16] Tanaka, K., Uchida, K., Ogimi, K., *et al.*: 'Optimal operation by controllable loads based on smart grid topology considering insolation forecasted error', *IEEE Trans. smart grid*, 2011, **2**, (3), pp. 438–444

[17] Meng, K., Wang, D., Dong, Z.Y., *et al.*: 'Distributed control of thermostatically controlled loads in distribution network with high penetration of solar PV', *CSEE J. Power Energy Syst.*, 2017, **3**, (1), pp. 53–62

[18] Xu, Y., Ma, J., Dong, Z.Y., *et al.*: 'Robust transient stability-constrained optimal power flow with uncertain dynamic loads', *IEEE Trans. Smart Grid*, 2017, **8**, (4), pp. 1911–1921

[19] Liu, J., Chen, H., Zhang, W., *et al.*: 'Energy management problems under uncertainties for grid-connected microgrids: a chance constrained programming approach', *IEEE Trans. Smart Grid*, 2017, **8**, (6), pp. 2585–2596

[20] Xiang, Y., Liu, J., Liu, Y.: 'Robust energy management of microgrid with uncertain renewable generation and load', *IEEE Trans. Smart Grid*, 2016, **7**, (2), pp. 1034–1043

[21] Jabr, R.A.: 'Robust transmission network expansion planning with uncertain renewable generation and loads', *IEEE Trans. Power Syst.*, 2013, **28**, (4), pp. 4558–4567

[22] Haghghat, H., Zeng, B.: 'Distribution system reconfiguration under uncertain load and renewable generation', *IEEE Trans. Power Syst.*, 2016, **31**, (4), pp. 2666–2675

[23] Ding, T., Liang, H., Xu, W.: 'An analytical method for probabilistic modeling of the steady-state behavior of secondary residential system', *IEEE Trans. Smart Grid*, 2017, **8**, (6), pp. 2575–2584

[24] Fischer, D., Stephen, B., Flunk, A., *et al.*: 'Modelling the effects of variable tariffs on domestic electric load profiles by use of occupant behavior submodels', *IEEE Trans. Smart Grid*, 2017, **8**, (6), pp. 2685–2693

[25] Shafie-khah, M., Siano, P.: 'A stochastic home energy management system considering satisfaction cost and response fatigue', *IEEE Trans. Ind. Inf.*, 2018, **14**, (2), pp. 629–638

[26] Du, Y., Jiang, L., Li, Y., *et al.*: 'A robust optimization approach for demand side scheduling under energy consumption uncertainty of manually operated appliances', *IEEE Trans. Smart Grid*, 2018, **9**, (2), pp. 743–755

[27] Blanco, I., Morales, J.M.: 'An efficient robust solution to the two-stage stochastic unit commitment problem', *IEEE Trans. Power Syst.*, 2017, **32**, (6), pp. 4477–4488

[28] Chen, Z., Wu, L., Shahidehpour, M.: 'Effective load carrying capability evaluation of renewable energy via stochastic long-term hourly based SCUC', *IEEE Trans. Sustain. Energy*, 2015, **6**, (1), pp. 188–197

[29] Xie, Y., Liao, S., Yuan, B., *et al.*: 'Fully-parallel area-efficient deep neural network design using stochastic computing', *IEEE Trans. Circuits Syst. II, Express Briefs*, 2017, **64**, (12), pp. 1382–1386

[30] Khanabadi, M., Fu, Y., Gong, L.: 'A fully parallel stochastic multiarea power system operation considering large-scale wind power integration', *IEEE Trans. Sustain. Energy*, 2018, **9**, (1), pp. 138–147

[31] Wu, T., Venkatasubramanian, V.M., Pothan, A.: 'Fast parallel stochastic subspace algorithms for large-scale ambient oscillation monitoring', *IEEE Trans. Smart Grid*, 2017, **8**, (3), pp. 1494–1503

[32] Fu, Y., Liu, M., Li, L.: 'Multiobjective stochastic economic dispatch with variable wind generation using scenario-based decomposition and asynchronous block iteration', *IEEE Trans. Sustain. Energy*, 2016, **7**, (1), pp. 139–149

[33] Santos, T.N., Diniz, A.L., Borges, C.L.T.: 'A new nested benders decomposition strategy for parallel processing applied to the hydrothermal scheduling problem', *IEEE Trans. Smart Grid*, 2017, **8**, (3), pp. 1504–1512

[34] Bolognani, S., Zampieri, S.: 'On the existence and linear approximation of the power flow solution in power distribution networks', *IEEE Trans. Power Syst.*, 2016, **31**, (1), pp. 163–172

[35] Atwa, Y.M., El-Saadany, E.F., Salama, M.M.A., *et al.*: 'Adequacy evaluation of distribution system including wind/solar DG during different modes of operation', *IEEE Trans. Power Syst.*, 2011, **26**, (4), pp. 1945–1952

[36] Duffie, J.A., Beckman, W.A.: 'Solar engineering of thermal processes' (John Wiley & Sons, Hoboken, NJ, USA, 2013)

[37] Orgill, J.F., Hollands, K.G.T.: 'Correlation equation for hourly diffuse radiation on a horizontal surface', *Sol. Energy*, 1977, **19**, (4), pp. 357–359

[38] Bracale, A., Caramia, P., Carpinelli, G., *et al.*: 'A Bayesian method for short-term probabilistic forecasting of photovoltaic generation in smart grid operation and control', *Energies*, 2013, **6**, (2), pp. 733–747

[39] Liu, S., Liu, P.X., Wang, X.: 'Stability analysis of grid-interfacing inverter control in distribution systems with multiple photovoltaic-based distributed generators', *IEEE Trans. Ind. Electron.*, 2016, **63**, (12), pp. 7339–7348

[40] Tan, Y.T., Kirschen, D.S., Jenkins, N.: 'A model of PV generation suitable for stability analysis', *IEEE Trans. Energy Convers.*, 2004, **19**, (4), pp. 748–755

[41] Hoke, A., Brissette, A., Smith, K., *et al.*: 'Accounting for lithium-ion battery degradation in electric vehicle charging optimization', *IEEE J. Top. Emerg. Sel. Top. Power Electron.*, 2014, **2**, (3), pp. 691–700

[42] Jiang, C.: 'A probabilistic bottom-up technique for modeling and simulation of residential distributed harmonic sources', PhD thesis, 2012

- [43] Zimmermann, J.-P., Evans, M., Griggs, J., *et al.*: 'Household electricity survey: a study of domestic electrical product usage', Intertek Testing & Certification Ltd., 2012
- [44] Birge, J.R., Rosa, C.H.: 'Parallel decomposition of large-scale stochastic nonlinear programs', *Ann. Oper. Res.*, 1996, **64**, (1), pp. 39–65
- [45] Berkelaar, M., Eikland, K., Notebaert, P.: 'LP solve reference guide menu'. Available at <http://lpsolve.sourceforge.net/5.5>, 2018
- [46] Wang, Y., Liang, H., Dinavahi, V.: 'Two-stage stochastic demand response in smart grid considering random appliance usage patterns', *IET Gener. Transm. Distrib.*, 2018, **12**, (18), pp. 4163–4171
- [47] Fact sheet: community energy storage for grid support. Available at <https://www.energy.gov/sites/prod/files/DTE.pdf>, October 2012
- [48] Hourly Ontario energy price (HOEP). Available at <http://www.ieso.ca/power-data/price-overview/hourly-ontario-energy-price>, April 2018
- [49] Time of use (TOU) price for residents and small businesses. Available at <http://www.ieso.ca/power-data/price-overview/time-of-use-rates>, May 2017 to April 2018
- [50] Feed-in-tariff (FIT) program. Available at <http://www.ieso.ca/sector-participants/feed-in-tariff-program/overview>, December 2016
- [51] PES test feeder. Available at <http://sites.ieee.org/pes-testfeeders/resources>, 2017
- [52] Kashem, M.A., Ganapathy, V., Jasmon, G.B., *et al.*: 'A novel method for loss minimization in distribution networks'. Proc. Int. Conf. Electric Utility Deregulation Restructuring Power Technologies Proc., 2000, pp. 251–256
- [53] Zhang, D., Fu, Z., Zhang, L.: 'An improved TS algorithm for loss-minimum reconfiguration in large-scale distribution systems', *Electr. Power Syst. Res.*, 2007, **77**, (5–6), pp. 685–694

READ ONLY